



## Effect of Varying Electrolyte Conductivity on the Electrochemical Behavior of Porous Electrodes

Vinten D. Diwakar\* and Venkat R. Subramanian\*\*z

Department of Chemical Engineering, Tennessee Technological University, Cookeville, Tennessee 38505, USA

Ionic conductivity in the air cathode of a polymer electrolyte membrane (PEM) fuel cell changes with distance depending on the ionomer loading [*J. Electrochem. Soc.*, **150**, A1440 (2003)]. When the ionic conductivity changes with distance inside a porous electrode, existing models in the literature fail to capture the behavior of porous electrodes. In this paper, we show how existing models in the literature can be modified to take care of varying ionic conductivity. The modified model is shown to be efficient in handling mathematical singularity arising from the distribution of ionic conductivity inside a porous electrode. In addition, the model developed was used to optimize the functionality of ionic conductivity (ionomer loading) to minimize the ohmic drop across a porous electrode. It is shown that depending on the system parameters, there might be an optimum way to distribute the ionomer loading inside the PEM fuel cell cathode.

© 2005 The Electrochemical Society. [DOI: 10.1149/1.1890725] All rights reserved.

Manuscript submitted September 21, 2004; revised manuscript received November 30, 2004.  
Available electronically April 1, 2005.

Macroscopic models based on porous electrode theory have been used to model, analyze, and simulate various electrochemical power sources (batteries, fuel cells, capacitors).<sup>1-5</sup> These models<sup>2-30</sup> are used for different purposes, including understanding the physics, predicting the experimental data, optimizing systems parameters, predicting thermal behavior, optimizing cell design, etc. Of late, macroscopic models have been used to model, simulate, and analyze ac impedance data of batteries and polymer electrolyte membrane (PEM) fuel cells.<sup>6,7,10-30</sup> Some researchers have used these models to estimate transport and kinetic parameters and ac impedance models.<sup>7,8</sup>

Recently, Guo *et al.*<sup>31</sup> analyzed ac impedance response of PEM fuel cell cathode for different distributions of ionomer loading. They assumed that the ionic conductivity inside the cathode varies as a product of effective ionic conductivity  $\kappa_0$  and the distribution function  $f(x) = x^n$ . For the functionality assumed by them, a mathematical singularity occurs in the boundary condition (at the current collector,  $x = 0$ ). In this paper, we present an alternate method of solving the problem by handling the singularity. The later part of the paper presents a method to find an optimum conductivity profile for minimizing the ohmic drop across the porous electrode.

### Mathematical Model

The cathode region of a PEM fuel cell is modeled in this paper. The geometry modeled is shown in Fig. 1.<sup>1</sup> The following assumptions are made: (i) the solid-phase potential is constant and zero; (ii) linear kinetics is valid, which is especially true for the case of ac impedance and high values of exchange current density; (iii) concentration gradients are absent; and (iv) the process is assumed to be at steady state.

The electrolyte current is governed by Ohm's law<sup>1</sup>

$$i_2 = -\kappa \frac{d\Phi_2}{dx} \quad [1]$$

where  $i_2$  is the electrolyte current density,  $\Phi_2$  is the electrolyte phase potential,  $\kappa$  is the ionic conductivity, and  $x$  is the distance from the current collector. Assuming linear kinetics, the gradient of current density is given by<sup>1</sup>

$$\frac{di_2}{dx} = -\frac{ai_0F}{RT}\Phi_2 \quad [2]$$

where  $a$  is the surface area per unit volume,  $\text{cm}^2/\text{cm}^3$ ,  $i_0$  is the exchange current density of the rate-determining step,  $\text{A}/\text{cm}^2$ ,  $F$  is

the Faraday's constant (96,487 C/mol),  $R$  is the universal gas constant, and  $T$  is the temperature in Kelvin. Combining Eq. 1 and 2, the governing equation for the electrolyte potential is obtained as

$$\kappa \frac{d^2\Phi_2}{dx^2} + \frac{d\kappa}{dx} \frac{d\Phi_2}{dx} = \frac{ai_0F}{RT}\Phi_2 \quad [3]$$

The conductivity,  $\kappa$ , changes with distance and is taken as a product of the effective ionic conductivity  $\kappa_0$  and a distribution function  $f(x)$

$$\kappa = \kappa_0 f(x) \quad [4]$$

Substituting Eq. 4 in 3 we get

$$\kappa_0 f(x) \frac{d^2\Phi_2}{dx^2} + \kappa_0 \frac{df(x)}{dx} \frac{d\Phi_2}{dx} = \frac{ai_0F}{RT}\Phi_2 \quad [5]$$

At the current collector the applied current is carried by solid phase (electrolyte current = 0), hence the potential gradient was taken as zero by Guo *et al.*<sup>31</sup>

$$x = 0, \quad -f(x) \frac{d\Phi_2}{dx} = 0 \quad [6]$$

At the porous electrode/electrolyte interface, the applied current is carried by the electrolyte (Eq. 1 and 4, Guo *et al.*<sup>31</sup>)

$$x = L, \quad -k_0 f(x) \frac{d\Phi_2}{dx} = i_{\text{app}} \quad [7]$$

In our paper, the distribution function  $f(x)$  is taken as

$$f(x) = (1 + n)x^n \quad [8]$$

The distribution function  $f(x)$  is taken in such a way that the average of  $f(x)$  is 1 and the average conductivity is  $\kappa_0$ , irrespective of the value of  $n$ . In Fig. 2,  $f(x)$  is plotted for different values of  $n$ .

Equation 5 can be solved with the boundary conditions (Eq. 6 and 7) for the electrolyte potential. However, we observe that in Eq. 6 if  $f(x) = 0$  at  $x = 0$  (as in Eq. 8) then  $d\Phi_2/dx$  may or may not be zero. Because  $f(x) = 0$  in Eq. 6, boundary condition Eq. 6 is true irrespective of the value of the potential gradient. Equation 6 is always satisfied and cannot be used as a boundary condition for the electrolyte potential  $\Phi_2$ . In this situation, we have a conductivity distribution which forces  $f(x) = 0$  in Eq. 6. Alternatively, in this paper we solve for the electrolyte current density instead of solving for the electrolyte potential,  $\Phi_2$ . Electrolyte current is given by Ohm's law (Eq. 1). Differentiating Eq. 2 and eliminating the potential gradient from Eq. 1 and 2 we obtain

\* Electrochemical Society Student Member.

\*\* Electrochemical Society Active Member.

z E-mail: vsubramanian@tntech.edu

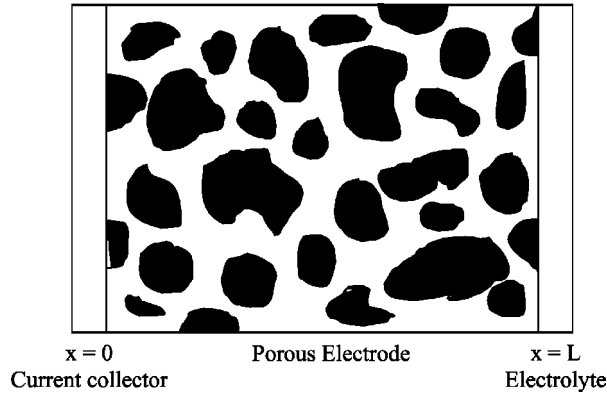


**Figure 1.** The geometry which is being modeled. The diagram shows that at boundary  $x = 0$  we have the current collector/porous electrode interface, and at boundary  $x = L$  we have the porous electrode/electrolyte interface.

$$f(x) \frac{d^2 i_2}{dx^2} = \left( \frac{a i_0 F}{RT \kappa_0} \right) i_2 \quad [9]$$

At the current collector the electrolyte phase current is zero

$$i_2 = 0 \text{ at } x = 0 \quad [10]$$

At the porous electrode/electrolyte interface the applied current is carried by the electrolyte

$$i_2 = i_{\text{app}} \text{ at } x = L \quad [11]$$

For convenience, the following dimensionless variables are introduced

$$I_2 = \frac{i_2}{i_{\text{app}}}; X = \frac{x}{L}; \Psi_2 = \frac{a i_0 F L}{RT i_{\text{app}}} \Phi_2 \quad [12]$$

where  $I_2$  is the dimensionless electrolyte current density,  $X$  is the dimensionless distance, and  $\Psi_2$  is the dimensionless electrolyte potential. The governing equation (Eq. 9) can be rewritten in terms of dimensionless variables as

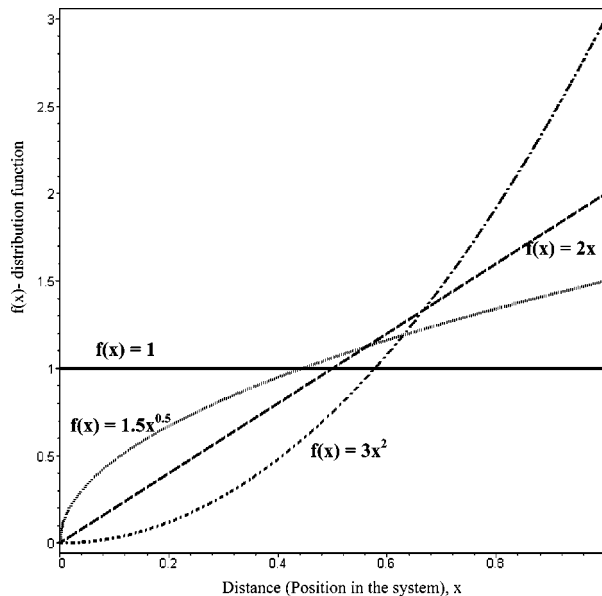


**Figure 2.** The distribution function  $f(x)$  which is  $(n+1)x^n$  is plotted as a function of distance (position in the system)  $x$ . The average  $f(x)$  was 1.

$$f(X) \frac{d^2 I_2}{dX^2} - v^2 I_2 = 0 \quad [13]$$

where  $v^2$  is the dimensionless current density and is given by

$$v^2 = \frac{a i_0 F L^2}{RT \kappa_0} \quad [14]$$

Now the boundary conditions are

$$I_2(0) = 0 \quad [15]$$

$$I_2(1) = 1 \quad [16]$$

In the governing equation (Eq. 13),  $f(X)$  in general takes the form  $(n+1)X^n$ . The governing equation, Eq. 13, can now be rewritten as

$$\frac{d^2 I_2(X)}{dX^2} - \frac{v^2 I_2(X)}{X^n(n+1)} = 0 \quad [17]$$

The general solution to the governing equation, Eq. 17, is given by<sup>9</sup>

$$I_2(X) = c_1 \sqrt{X} \text{Bessel}J \left( -\frac{1}{-2+n}, \frac{2\sqrt{-\frac{v^2}{n+1}} X^{(1-n/2)}}{-2+n} \right) + c_2 \sqrt{X} \text{Bessel}Y \left( -\frac{1}{-2+n}, \frac{2\sqrt{-\frac{v^2}{n+1}} X^{(1-n/2)}}{-2+n} \right) \quad [18]$$

Depending on the values of  $n$ , the constants  $c_1$  and  $c_2$  can be solved using boundary conditions 15 and 16

$$I_2(X) = \frac{\sqrt{X} \text{Bessel}J \left( -\frac{1}{-2+n}, \frac{2\sqrt{-\frac{v^2}{n+1}} X^{(1-n/2)}}{-2+n} \right)}{\text{Bessel}J \left( -\frac{1}{-2+n}, \frac{2\sqrt{-\frac{v^2}{n+1}}}{-2+n} \right)} n < 2 \quad [19]$$

and

$$I_2(X) = \frac{\sqrt{X} \text{Bessel}K \left( \frac{1}{-2+n}, \frac{2v}{\sqrt{n+1} X^{(-1+n/2)}} \right)}{\text{Bessel}K \left( \frac{1}{-2+n}, \frac{2v}{\sqrt{n+1}} \right)} n > 2 \quad [20]$$

For  $n = 0$ , both Eq. 19 and 20 reduce to the expected expression for constant conductivity<sup>1</sup>

$$I_2(X)_{n=0} = \frac{\sinh(vX)}{\sinh(v)} \quad [21]$$

From the solution for the electrolyte current density  $I_2(X)$ , we can find the electrolyte potential  $\Psi_2(X)$  using the following equation

$$\frac{dI_2(X)}{dX} = \Psi_2(X) \quad [22]$$

## Results and Discussion

In Fig. 3, dimensionless electrolyte current density distribution is plotted for different values of exponent  $n$ . When  $n$  is 0 or 1, the profile is almost linear and as  $n$  increases we observe a steep gradient in the distribution of current density. In Fig. 4, dimensionless electrolyte potential is plotted as a function of dimensionless dis-

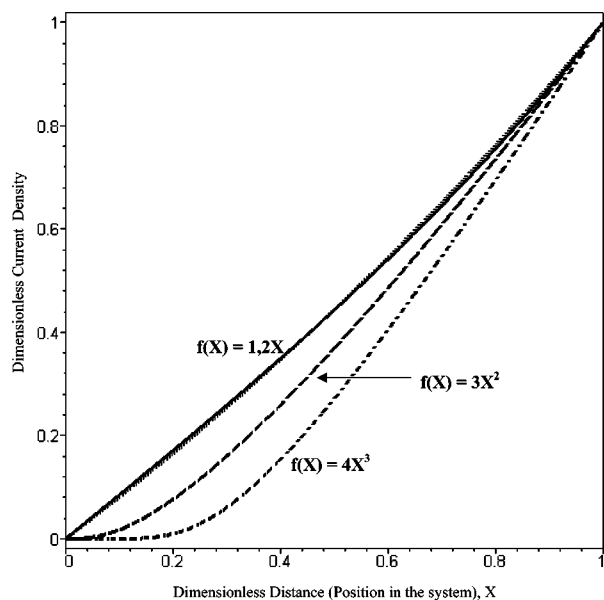


**Figure 3.** Current density distribution. The dimensionless current density is plotted as a function of dimensionless distance ( $X$ ).

tance ( $X$ ), from the current collector for different values of exponent  $n$ . When  $n = 3$ , the electrolyte potential is equal to zero at  $x = 0$  and for other values of  $n$  it is nonzero at  $x = 0$ .

Dimensionless potential gradient in Fig. 5 is plotted as a function of dimensionless distance  $X$  for different values of exponent  $n$ . When  $n$  is 0, the potential gradient is zero and it is nonzero for other values of  $n$ . Electrolyte potential gradient is not zero for other values of  $n$ , and this means that we cannot make the assumption that potential gradient is zero when ionic conductivity changes as a function of  $X$ . This shows that we cannot use Eq. 6 to model electrolyte potential.

Dimensionless electrolyte current density is plotted as a function of dimensionless distance  $X$  for different values of  $v$  in Fig. 6. We observe that as the dimensionless electrolyte exchange current den-

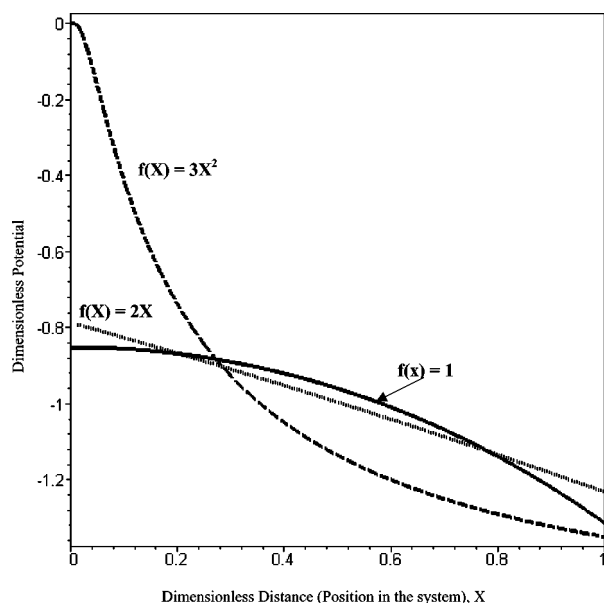


**Figure 4.** Potential distribution. The dimensionless potential is plotted as a function of dimensionless distance ( $X$ ).

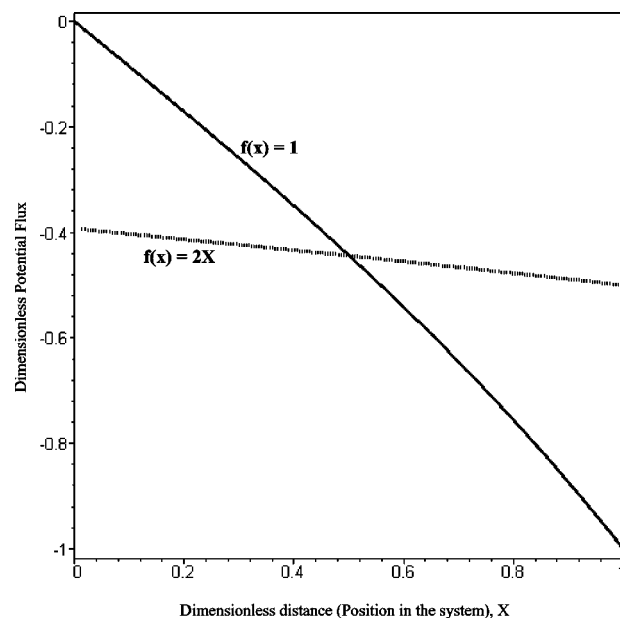


**Figure 5.** Dimensionless potential flux as a function of dimensionless distance (position in the system) ( $X$ ).

sity  $v$  increases, the dimensionless electrolyte current density becomes more nonuniform. Dimensionless electrolyte potential is plotted as a function of dimensionless distance  $X$  for different  $v$  for a particular value of  $n$  ( $n = 1$ ) in Fig. 7. As  $v$  increases, the distribution becomes more nonuniform. The dimensionless electrolyte potential is plotted as a function of the dimensionless distance in Fig. 8 with a constant case of dimensionless electrolyte exchange current density  $v$  ( $v = 1$ ) for varying values of  $n$ . It is interesting to observe that the change in dimensionless electrolyte potential across the dimensionless distance  $X$  increases as  $n$  increases (the lines become steeper).

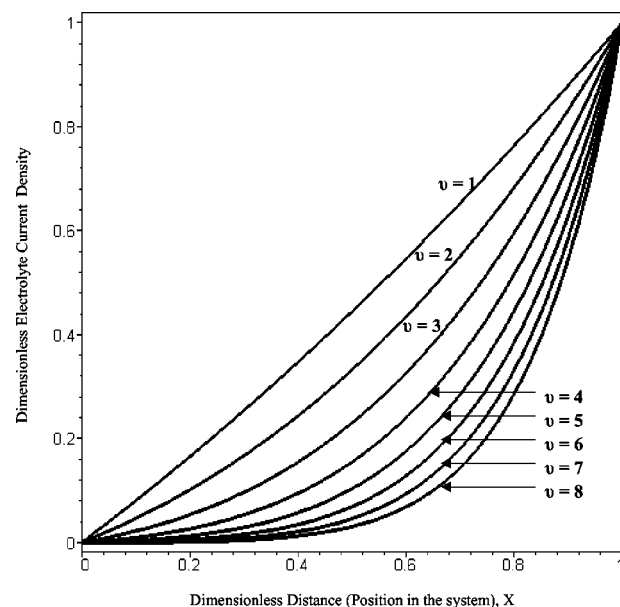


**Figure 6.** Plot of dimensionless electrolyte current density as a function of dimensionless distance (position in the system) ( $X$ ) for a constant value of  $n$  ( $n = 1$ ) and varying values of  $v$ .

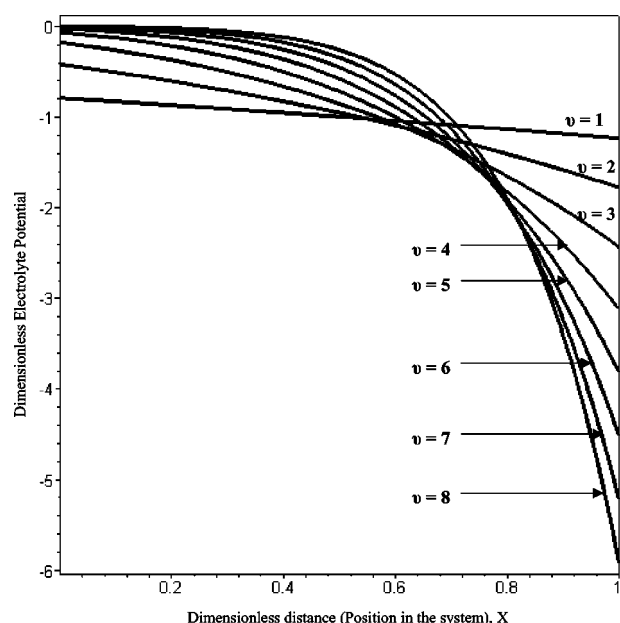


**Figure 7.** Plot of dimensionless electrolyte potential as a function of dimensionless distance (position in the system) ( $X$ ) for a constant value of  $n$  ( $n = 1$ ) and varying values of  $v$ .

### Optimum Conductivity Profile

If our objective is to minimize the ohmic drop across the electrode we can calculate it using the expression

$$\text{ohmic drop} = \text{abs}(\Psi_{2,x=1} - \Psi_{2,x=0}) \quad [23]$$

Dimensionless ohmic drop is plotted as a function of  $n$  for particular value of  $v$  (i.e., 0.1 and 1) in Fig. 9. We observe that for a particular value of system parameter  $v$ ,  $v = 1$ , there might be a minimum for the ohmic drop, and, for  $v = 0.1$ , we don't observe a minima. We conclude that depending on the system parameters, there might be an optimum conductivity profile to minimize the ohmic drop. Note that the function  $f(x)$  was chosen such that irrespective of the value of  $n$ , the average conductivity remains the same and is equal to  $\kappa_0$ . For a given average  $\kappa_0$  and a given value of  $v$  we can find an optimum  $n$  based on which we may be able to load the ionomer. Currently we are doing experiments in which membrane is loaded for different values of  $n$  in Eq. 8 to optimize the ohmic drop across the membrane (note that  $v$  can be changed by changing the thickness

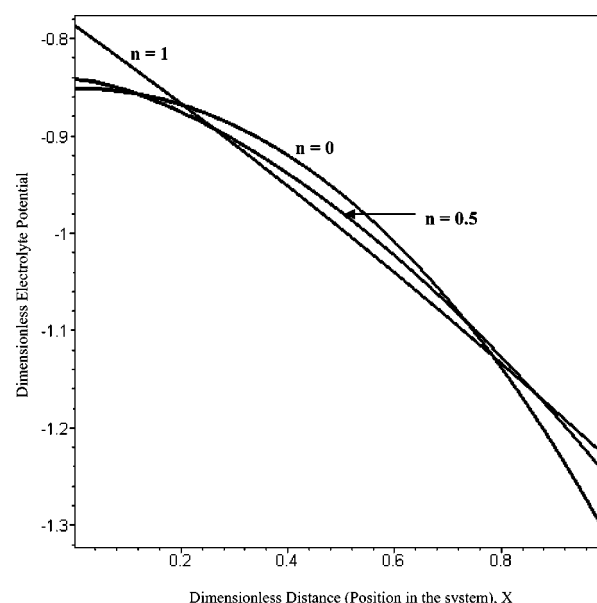


**Figure 8.** Plot of dimensionless electrolyte potential as a function of dimensionless distance (position in the system) ( $X$ ) for a constant value of  $v$  ( $v = 1$ ) and varying values of  $n$ . The shape of the curve depends on  $n$ .

or length  $L$  as defined in Eq. 14), and comparison of experiments with the model developed in this paper will be communicated later.

### Conclusions

In this paper, an alternate method is presented to obtain the potential and current density distributions for porous electrodes with space-varying ionic conductivity. The method presented handles the inherent singularity in one of the boundary conditions. The governing equations to be solved for are written in terms of the electrolyte current density  $i_2$ . A method to find the optimum conductivity profile is also presented.

Future work includes similar models for lithium-ion batteries especially during high discharge rates when the electrolyte concentration approaches zero. It will be more efficient to simulate for the electrolyte current density  $i_2$ , instead of the electrolyte potential  $\Phi_2$ , because we are avoiding the mathematical singularity. Only linear kinetics is assumed in this paper; Butler-Volmer kinetics will be included for more practical applications.

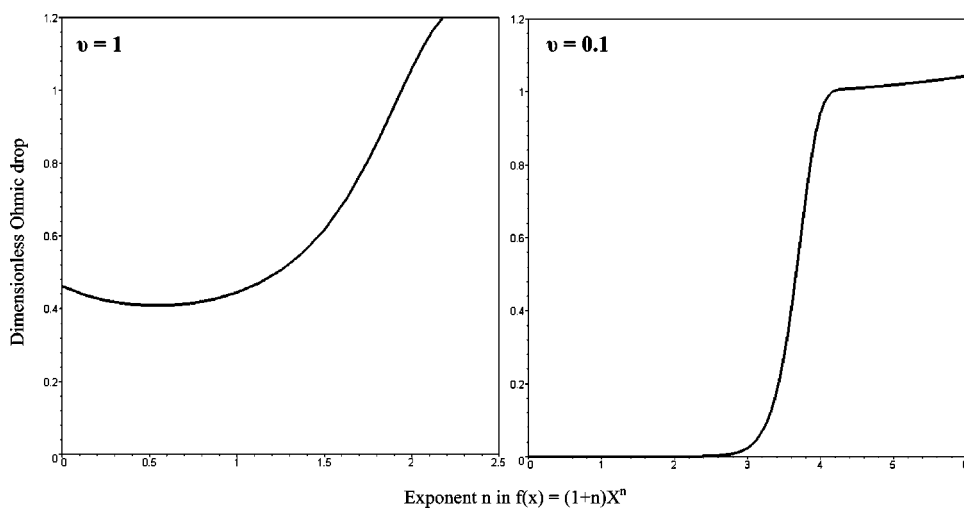


**Figure 9.** Plot of dimensionless ohmic drop as a function of exponent  $n$  in  $f(X) = (n + 1)X^n$  for a constant value of  $v$  ( $v = 1$  and  $v = 0.1$ ). The shape of the curve depends on  $n$ .

In this paper we have modeled just the electrolyte phase without other processes. The next step is to use a rigorous model in which  $i_2$  will be solved instead of  $\Phi_2$ . This approach will be extended for modeling ac impedance in the future.

#### Acknowledgment

The authors acknowledge the Center for Electric Power, Tennessee Technological University for the graduate research assistantship provided to V.D.D.

*Tennessee Technological University assisted in meeting the publication costs of this article.*

#### References

1. J. S. Newman, *Electrochemical Systems*, 2nd ed., Prentice Hall, Englewood Cliffs, NJ (1991).
2. M. Perry, J. Newman, and E. J. Cairns, *J. Electrochem. Soc.*, **145**, 5 (1998).
3. M. Doyle, T. J. Fuller, and J. Newman, *J. Electrochem. Soc.*, **140**, 1526 (1993).
4. G. G. Botte, V. R. Subramanian, and R. E. White, *Electrochim. Acta*, **45**(15-16), 2595 (2000).
5. P. Gomadam, J. W. Weidner, T. A. Zawodzinski, and A. P. Saab, *J. Electrochem. Soc.*, **150**, E371 (2003).
6. Q. Guo, V. R. Subramanian, J. W. Weidner, and R. E. White, *J. Electrochem. Soc.*, **149**, A307 (2002).
7. Q. Guo and R. E. White, *J. Electrochem. Soc.*, **151**, E133 (2004).
8. S. Motupally, C. C. Streinz, and J. W. Weidner, *J. Electrochem. Soc.*, **142**, 1401 (1995).
9. R. G. Rice and D. D. Do, *Applied Mathematics and Modeling for Chemical Engineers*, John Wiley, NY (1995).
10. T. F. Fuller, M. Doyle, and J. Newman, *J. Electrochem. Soc.*, **141**, 1 (1994).
11. T. F. Fuller, M. Doyle, and J. Newman, *J. Electrochem. Soc.*, **141**, 982 (1994).
12. M. Doyle, T. F. Fuller, and J. Newman, *Electrochim. Acta*, **39**, 2073 (1994).
13. J. Newman, *J. Electrochem. Soc.*, **142**, 97 (1995).
14. W. Tiedemann and J. Newman, *J. Electrochem. Soc.*, **142**, 1054 (1995).
15. M. Doyle and J. Newman, *J. Power Sources*, **54**, 46 (1995).
16. Y. Ma, M. Doyle, T. F. Fuller, M. M. Doeff, L. C. De Jonghe, and J. Newman, *J. Electrochem. Soc.*, **142**, 1859 (1995).
17. C. R. Pals and J. Newman, *J. Electrochem. Soc.*, **142**, 3274 (1995).
18. C. R. Pals and J. Newman, *J. Electrochem. Soc.*, **142**, 3282 (1995).
19. M. Doyle and J. Newman, *Electrochim. Acta*, **40**, 2191 (1995).
20. M. Doyle, A. S. Gozdz, C. N. Schmutz, J.-M. Tarascon, and J. Newman, *J. Electrochem. Soc.*, **143**, 1890 (1996).
21. M. Doyle and J. Newman, *J. Appl. Electrochem.*, **27**(7), 846 (1997).
22. R. M. Darling and J. Newman, *J. Electrochem. Soc.*, **144**, 3057 (1997).
23. W. Tiedemann and J. Newman, *J. Electrochem. Soc.*, **144**, 3081 (1997).
24. M. Doyle, J. P. Meyers, and J. Newman, *J. Electrochem. Soc.*, **147**, 99 (2000).
25. J. P. Meyers, M. Doyle, R. M. Darling, and J. Newman, *J. Electrochem. Soc.*, **147**, 2930 (2000).
26. H. Hafezi and J. Newman, *J. Electrochem. Soc.*, **147**, 3036 (2000).
27. P. Arora, M. Doyle, A. S. Gozdz, R. E. White, and J. Newman, *J. Power Sources*, **88**, 219 (2000).
28. J. P. Meyers and J. Newman, *J. Electrochem. Soc.*, **149**, A710 (2002).
29. J. P. Meyers and J. Newman, *J. Electrochem. Soc.*, **149**, A718 (2002).
30. J. P. Meyers and J. Newman, *J. Electrochem. Soc.*, **149**, A729 (2002).
31. Q. Guo, M. Cayetano, Y.-M. Tsou, E. S. De Castro, and R. E. White, *J. Electrochem. Soc.*, **150**, A1440 (2003).